

## Controlled interactions of femtosecond light filaments in air

Bonggu Shim, Samuel E. Schrauth, Christopher J. Hensley, Luat T. Vuong, Pui Hui, Amiel A. Ishaaya, and Alexander L. Gaeta\*

*School of Applied and Engineering Physics, Cornell University, Ithaca, New York 14853, USA*

(Received 19 April 2009; revised manuscript received 25 May 2010; published 28 June 2010)

We experimentally demonstrate coherent control of two light filaments in air generated by ultrafast laser pulses, as proposed by Xi *et al.* [*Phys. Rev. Lett.* **96**, 025003 (2006)]. We show that depending on the relative phase and the incidence angle, the filaments can experience fusion, repulsion, energy redistribution, and spiral motion for propagation in air. By translating the initial beams on subwavelength scales, we achieve  $\sim 1$ -mm transverse deflection of approximately 0.5-mJ energy for parallel propagation and  $7^\circ$  angular deflection for spiral motion in 3-m propagation. Our approach using the relative beam phases to reliably control propagation of femtosecond light filaments is potentially applicable to remote sensing and lightning guiding.

DOI: [10.1103/PhysRevA.81.061803](https://doi.org/10.1103/PhysRevA.81.061803)

PACS number(s): 42.65.Sf, 42.65.Tg, 42.65.Jx

Since Braun *et al.* [1] and others [2,3] observed self-channeling beams in air with high-power femtosecond pulses, this subject has drawn significant attention for its potential applications to lightning guiding, remote sensing, pulse compression [4–12], and recently, THz generation [13]. Filamentation occurs when high-power beams undergoing self-focusing by Kerr-lensing are balanced by diffraction and/or plasma defocusing, and theoretical simulations are able to describe this remarkable self-channeling phenomenon with reasonable accuracy [10,11].

Various experiments have investigated the spatial dynamics of filament formation in air, including fusion of and competition between multiple filaments [14,15]. The use of masks, pinholes, and beam shaping have been shown to control the formation of multiple filaments with single beams [16–18]. For two-beam experiments, THz signal enhancement in air by controlling time delays between two filaments [19], steering of a probe (filament) in the tens of femtosecond time scale by periodic molecular wakes induced by a pump filament [20], and energy exchange between two crossing beams via control of chirps and time delays [21] have been demonstrated. Recently, numerical simulations [22] suggest that two light filaments in air can be phase controlled (subwavelength delay) both for parallel and nonparallel propagation in a manner similar to soliton interactions [23]. Although fusion and competition of collapsing light beams have been demonstrated in a parallel propagation configuration in short Kerr media (BK7) [24], phase-controlling experiments have not yet been realized using self-channeling beams in air.

In this Rapid Communication, we report on the first experimental verification of phase control of two air filaments in which we investigate coherent control of parallel and spiral propagation between the filaments. We are able to demonstrate fusion, repulsion, energy transfer, and spiral motion by changing the relative phase and the crossing angle, as theoretically predicted by Xi *et al.* [22]. In particular, compared with the spiraling of incoherent solitons in which the force is always attractive [23], here we present coherently controlled spiral propagation between two air filaments without fusion using

precise phase control. We expect that our method can be applied to controlling long-range propagation of femtosecond light filaments including remote sensing and lightning guiding.

In our experiments, Ti:sapphire laser pulses (0.5 TW peak power, <5% shot-to-shot energy fluctuation, 10-Hz repetition rate, 800 nm, and 50 fs) are split into two arms. We limit the maximum energy of each arm to 2 mJ (40 GW) to avoid multifilamentation. In one arm, we employ a motorized delay stage and a half-wave plate to control the relative phase and polarization. Two beams are interferometrically recombined by a beam splitter whereby the spatial separation between the arms is controllable. A mirror telescope is subsequently employed to resize both beams to a  $800\text{-}\mu\text{m}$  average spot size. We measure the single-shot, self-channeling mode profiles at different distances using the front surface reflection of a BK7 glass wedge and a 12-bit charge-coupled device (CCD) camera with a  $f/3$  achromatic lens. The maximum propagation distance is 3 m, and the  $800\text{-}\mu\text{m}$  spot size ( $1/e^2$  radius) corresponds to a  $2.5\text{-m}$  Rayleigh range.

The spot size for a single beam as a function of propagation distance for different powers is obtained by blocking one arm of the interferometer (Fig. 1). When the peak power is 20 GW, which corresponds to approximately twice the critical power ( $P_{cr} = 10$  G) for self-focusing [1,25], an air filament forms with a  $500\text{-}\mu\text{m}$  radius after 1.5 m of propagation [Figs. 1(a) and 1(b)]. The 40-GW beam decreases to a  $250\text{-}\mu\text{m}$  radius at 1.3 m and slightly diffracts at longer distances. For comparison, a collimated, low-power 4-MW power beam expands to  $1000\text{ }\mu\text{m}$  horizontally and  $800\text{ }\mu\text{m}$  vertically because of diffraction [Figs. 1(a) and 1(b)]. For the two-filament interaction experiments, each beam contains 20 GW of peak power.

Although the propagation distance is limited to 3 m due to laboratory space, other groups have measured large air filaments of  $\sim 1$  mm diameter with relatively weak intensities ( $10^{11}\text{--}10^{12}$  W/cm<sup>2</sup>) using collimated beams [14,26–29], which are comparable in size to the beam in our measurements. Figure 1(c) shows examples of spatial profiles at different locations. The initially asymmetric beam evolves to a symmetric Townes-like profile [30–32] as it self-focuses in air and is subsequently balanced mostly by diffraction. Based on the energy fluence measurement within the  $1/e^2$  diameter of the

\*a.gaeta@cornell.edu

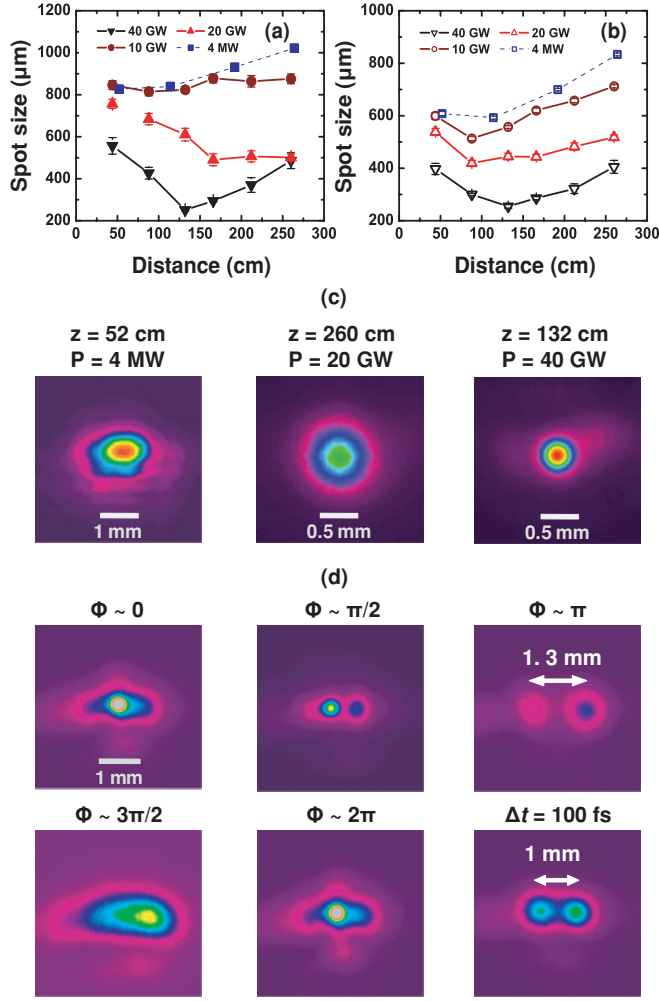


FIG. 1. (Color online) (a) Horizontal and (b) vertical spot sizes as functions of the propagation distance for different input powers. Each data point represents a 24-shot average. (c) Examples of mode profiles with different powers at different locations. (d) Mode profiles after 2.7-m propagation for two parallel beam interactions with different phases and for the case in which there is no temporal overlap. The peak power of each beam is 20 GW.

filament [33], we estimate the peak power to be 11.3 GW for the 20-GW beam, which agrees well with Ref. [33], and thus the peak intensity  $I_0$  is estimated to be less than  $3 \times 10^{12}$  W/cm<sup>2</sup>. As a result, we believe that the effects of multiphoton ionization (MPI) and plasma-induced defocusing are minimal in our case since this estimate is significantly less than  $10^{13}$  W/cm<sup>2</sup> at which MPI becomes important [14].

When two beams copropagate with parallel linear polarizations and 1-mm center-to-center separation, we observe that the self-channeling beams undergo fusion, repulsion, and energy transfer depending on the relative phase between the beams, in a manner similar to solitons [23] and to collapsing beams in solids [24]. Figure 1(d) shows the mode profiles after 2.7-m propagation distance. When the beams are in phase ( $\phi = 0$  and  $2\pi$ ), the nonlinear index change at the center becomes high because of constructive interference, and the beams attract each other via self-focusing and form a single filament. However, when the beams are initially out

of phase ( $\phi = \pi$ ), the index change at the center is lower because of destructive interference, which leads to an increase in separation ( $\Delta x = 1.3$  mm) and which is in contrast to the case where there is no temporal overlap ( $\Delta t = 100$  fs). For the cases of  $\phi = \pi/2$  and  $3\pi/2$ , energy transfer and redistribution of as much as 0.5 mJ of energy occurs between the two beams based on the fact that one filament contains approximately one critical power ( $P_{cr} = 10$  GW). The phase control is robust unless there is external perturbation such as vibration in an optical table.

To compare with experiments, we perform numerical simulations using the time-averaged (2D + 1) nonlinear Schrödinger equation (NLSE) in normalized units, which is given as [34,35]

$$\frac{\partial u}{\partial \zeta} = \frac{i}{4} \nabla_{\perp}^2 u + i\alpha \frac{L_{df}}{L_{nl}} |u|^2 u - i \frac{L_{df}}{L_{pl}} |u|^{2K} u - \frac{1}{2\sqrt{K}} \frac{L_{df}}{L_{mp}} |u|^{2(K-1)} u, \quad (1)$$

where  $u = E(\mu, \nu, \zeta)/E_0$  is the electric field amplitude normalized by the initial electric field amplitude,  $\zeta = z/L_{df}$  is the propagation distance normalized by the diffraction length  $L_{df} = \pi w_0^2/\lambda_0 = k_0 w_0^2/2$ ,  $k_0 = 2\pi/\lambda_0$  is the central wave number at 800 nm,  $\mu = x/w_0$  and  $\nu = y/w_0$  are the transverse coordinates normalized by the average spot size  $w_0$ ,  $K = 8$  is the number of photons for MPI of oxygen molecules,  $\nabla_{\perp}^2 = \partial^2/\partial\mu^2 + \partial^2/\partial\nu^2$  is the transverse Laplacian,  $\alpha = 0.375$  is the constant that takes into account the time-averaged Raman contribution to the nonlinear refractive index for  $\tau_0 = 50$  fs pulses,  $L_{nl} = (k_0 n_2 I_0)^{-1}$  is the nonlinear length,  $I_0$  is the peak input laser intensity,  $L_{pl} = (\gamma I_0^K)^{-1}$  is the plasma length,  $\gamma = \sqrt{\pi/8K} (T k_0 \sigma_K \rho_{at}) / 2\rho_{crit}$ ,  $T = 0.1\tau_0$  is the reduced pulse duration mainly due to MPI,  $\sigma_K = 2.88 \times 10^{-99}$  cm<sup>13</sup>/(W<sup>7</sup> s) is the MPI coefficient,  $\rho_{at} \simeq 5.4 \times 10^{18}$  cm<sup>-3</sup> is the density of oxygen molecules in air,  $\rho_{crit}$  is the critical density at 800 nm,  $L_{mp} = [\beta^{(K)} I_0^{(K-1)}]^{-1}$  is the  $K$ -photon absorption length, and  $\beta^{(K=8)} = 4.25 \times 10^{-98}$  cm<sup>13</sup>/W<sup>7</sup> is the eight-photon absorption coefficient. The terms on the right-hand side of the equation are associated with diffraction, self-focusing, plasma defocusing, and multiphoton absorption (MPA), respectively. Although this model ignores dispersion, which can be nonnegligible for propagation of high-intensity short pulses and collisional ionization, it effectively simulates beam profiles of air filaments and is computationally economical compared with full (3D + 1) simulations. Another factor that can potentially influence beam propagation by inducing beam asymmetry and the pointing instability is air turbulence [27,36–38]. However, as suggested by Roskey *et al.* [39], typical laboratory air turbulence has a negligible effect in our case because of the small beam size ( $\leq 1$  mm) and relatively short propagation distance ( $< 10$  m), which is corroborated by our measurements showing clean, symmetric beam profiles during filamentation [see Fig. 1(c)]. However, air turbulence in adverse weather conditions may provide some limitations to controlling the two beams in applications such as lightning guiding because of pointing instability. In our experiments, we can neglect the quantum wake effect [20] since the peak intensities are 1 order of magnitude smaller than those used in Ref. [20], which corresponds to an index response time

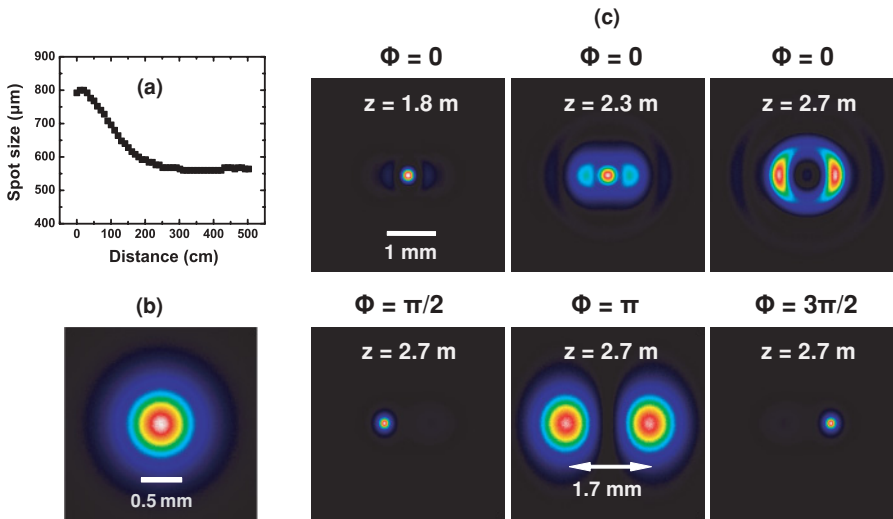


FIG. 2. (Color online) (a) Simulation results of spot size as a function of propagation distance for the 20-GW beam with  $P_{cr} = 7.5$  GW using the empirically modified time-averaged NLSE. (b) Mode profile of a single filament in the time-averaged NLSE. (c) Simulation results for two parallel beam interactions with different relative phases.

( $\sim 400$  fs) that is much larger than our pulse duration (50 fs) and delay ( $< 3$  fs) between two beams.

Since the beam size (i.e., intensity) is a critical parameter for two-beam interactions, we use a method of empirically changing the critical power  $P_{cr}$  within a reasonable range to match the measured beam sizes of a single filament with 20-GW power [see Figs. 1(a) and 1(b)]. Figure 2(a) shows the simulation result of spot size versus propagation distance with  $P_{cr} = 7.5$  GW. Here we assume that the initial laser field with 20-GW power has a  $800\text{-}\mu\text{m}$   $1/e^2$  radius with a symmetric Gaussian profile, and 10% noise is included in the simulation. As is shown, a nearly stable beam with a  $560\text{-}\mu\text{m}$  spot size [Fig. 2(b)] forms after 1.5-m propagation, which is comparable to the experimental results. For our simulations of the two-beam interaction, we will assume  $P_{cr} = 7.5$  GW, which corresponds to a relatively low intensity ( $5 \times 10^{12}$  W/cm $^2$ ) such that the filament is primarily due to a balance between diffraction and self-focusing.<sup>1</sup>

Numerical results simulating two copropagating beams with different phases are shown in Fig. 2(c) and qualitatively reproduce the experimental results at 2.7 m, with the exception of the zero-phase case. Although a single filament by fusion forms and propagates 2.7 m in the experiment, our simulation shows that the beam undergoes collapse at 1.8 m, and a spatial ring profile develops by MPA and plasma defocusing at longer distances for the zero-phase case [top row of Fig. 2(c)]. We believe the discrepancy between theory and experiment stems mainly from neglecting dispersion, which can prevent beam collapse by pulse splitting in the simulations [8,40,41].<sup>2</sup> Also, our empirically modified model does not reproduce the measurement quantitatively when there is energy exchange between two filaments, and thus the balance between self-focusing and diffraction is perturbed.

<sup>1</sup>Intuitively, the 20-GW power becomes one effective critical power in Eq. (1) for  $P_{cr} = 7.5$  GW, combined with the Raman factor ( $\alpha = 0.375$ ) ( $0.375 \times 20/7.5 \sim 1$ ).

<sup>2</sup>Although dispersion is negligible for 20-GW single beams, we measure pulse splitting for the zero-phase case, which can be explained only by including dispersion [10,11].

When two beams interact with a small converging incidence angle in different planes, an angular momentum is imparted, and the two in-phase filaments show spiral propagation since the attractive force between two filaments is compensated by the centrifugal force, as in the case of solitons [23]. Figure 3(a) shows that the degree of rotation is small ( $< 2^\circ$ ) at short distances (1.4 m). However, as the beams interact over a greater distance, the degree of rotation becomes larger with a maximum rotation of  $7^\circ$  with respect to the case of no temporal overlap. Here the incidence angle is about  $0.02^\circ$  only in the horizontal plane for both beams, and initial separations are

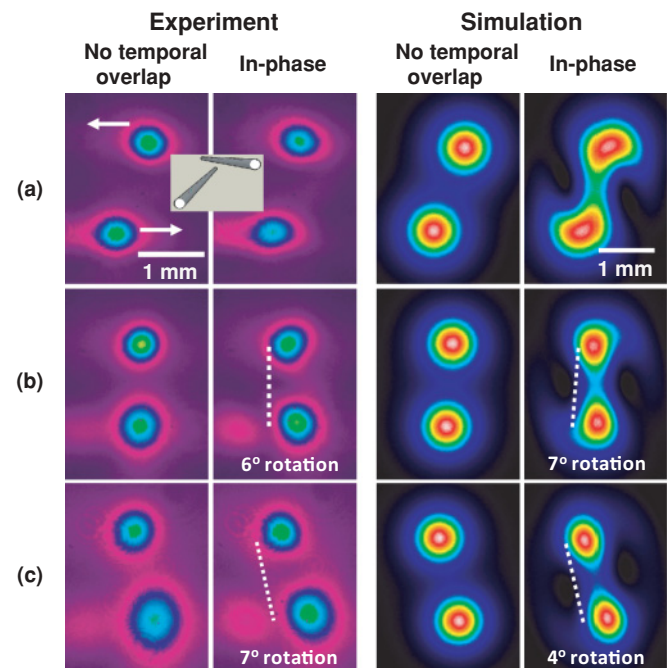


FIG. 3. (Color online) Experimental and calculated spiral motion (in phase) for interacting and noninteracting filaments for various propagation distances: (a) 1.4 m, (b) 2 m, and (c) 2.6 m. Dotted lines are references indicating axes for no temporal overlap cases. The incidence angle is  $0.02^\circ$  in the horizontal plane for both beams, and the initial separations are 1.5 mm horizontally and 1.4 mm vertically (inset). The peak power of each beam is 20 GW.



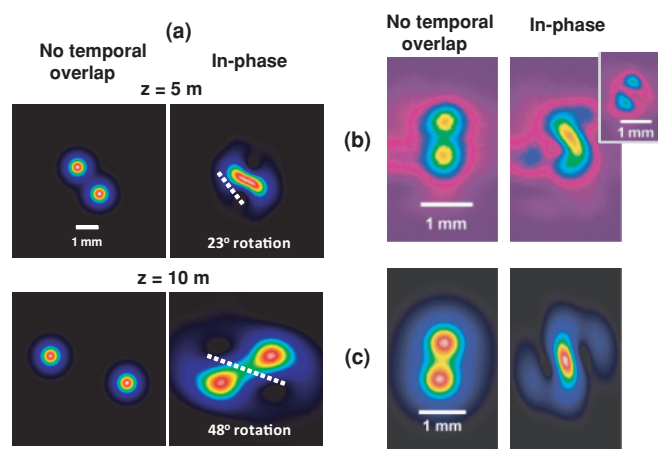


FIG. 4. (Color online) (a) Calculated spiral motion for longer propagation. The incidence angle is  $0.014^\circ$  only in the horizontal plane for both beams, and initial separations are 1.5 mm horizontally and 1.2 mm vertically. (b) Experimental (top row) and (c) calculated (bottom row) spiral motion with small vertical separation (0.8 mm) after 2-m propagation. The incidence angle and the horizontal separation are the same as in Fig. 3. The out-of-phase ( $\pi$  phase) case is shown as an inset.

1.5 mm horizontally and 1.4 mm vertically. Since there is little energy exchange between the two filaments for the spiral motion, the agreement between the simulation and the experiment is good. However, the small quantitative error may

be due to the difference in initial beam profiles and parameters such as initial separations and incidence angles.

Our calculation shows that larger rotation ( $48^\circ$ ) can be achieved at longer propagation distances with small incidence angles [Fig. 4(a)]. When the initial separation is smaller (0.8 mm vertically), the two filaments merge because of the stronger attractive force even though larger rotation is observed [Figs. 4(b) and 4(c)]. For comparison, when the beams are initially out of phase, the two filaments repel such that no fusion is observed, as shown in the inset to Fig. 4(b).

In conclusion, we demonstrate coherent phase control of filament interactions in air. The fusion, repulsion, energy transfer, and spiral propagation of two filaments are controlled by varying the relative phase and incidence angle. The simulations based on the empirically modified NLSE show good agreement with experimental results. Although the results described here correspond to propagation distances of  $\sim 3$  m, we believe that our approach, which is equally robust with the beam-steering method using the molecular quantum wake [20], can be extended to longer propagation distances ( $> 10$  m) with potential applications to lightning guiding and remote sensing.

This work was supported by the NSF under Grant No. PHY-0244995, the Army Research Office under Grant No. 48300-PH, and the Air Force Office for Scientific Research. The authors thank Y. Okawachi, M. Foster, P. Londero, and R. Frehlich for useful discussions.

- [1] A. Braun *et al.*, *Opt. Lett.* **20**, 73 (1995).
- [2] E. T. J. Nibbering *et al.*, *Opt. Lett.* **21**, 62 (1996).
- [3] A. Brodeur *et al.*, *Opt. Lett.* **22**, 304 (1997).
- [4] R. P. Ficher *et al.*, *IEEE Trans. Plasma Sci.* **35**, 1430 (2007); A. Houard *et al.*, *Appl. Phys. Lett.* **90**, 171501 (2007); J.-C. Diels *et al.*, *Sci. Am.* **277**, 50 (1997).
- [5] L. Wöste *et al.*, *Laser Optoelektron.* **29**, 51 (1997).
- [6] P. Rairoux *et al.*, *Appl. Phys. B* **71**, 573 (2000).
- [7] J. Kasparian *et al.*, *Science* **301**, 61 (2003).
- [8] A. L. Gaeta, *Science* **301**, 54 (2003).
- [9] S. L. Chin *et al.*, *Can. J. Phys.* **83**, 863 (2005), and references therein.
- [10] A. Couairon and A. Mysyrowicz, *Phys. Rep.* **441**, 47 (2007), and references therein.
- [11] L. Bergé *et al.*, *Rep. Prog. Phys.* **70**, 1633 (2007), and references therein.
- [12] J. Kasparian and J.-P. Wolf, *Opt. Express* **16**, 466 (2008).
- [13] C. D'Amico *et al.*, *Phys. Rev. Lett.* **98**, 235002 (2007).
- [14] S. Tzortzakakis *et al.*, *Phys. Rev. Lett.* **86**, 5470 (2001).
- [15] S. A. Hosseini *et al.*, *Phys. Rev. A* **70**, 033802 (2004).
- [16] G. Méchain, A. Couairon, M. Franco, B. Prade, and A. Mysyrowicz, *Phys. Rev. Lett.* **93**, 035003 (2004).
- [17] Z. Hao *et al.*, *Opt. Express* **15**, 16102 (2007).
- [18] G. Fibich *et al.*, *Opt. Lett.* **29**, 1772 (2004).
- [19] Y. Liu *et al.*, *Phys. Rev. Lett.* **99**, 135002 (2007).
- [20] S. Varma, Y. H. Chen, and H. M. Milchberg, *Phys. Rev. Lett.* **101**, 205001 (2008); F. Calegari *et al.*, *ibid.* **100**, 123006 (2008).
- [21] A. C. Bernstein, M. McCormick, G. M. Dyer, J. C. Sanders, and T. Ditmire, *Phys. Rev. Lett.* **102**, 123902 (2009).
- [22] T.-T. Xi, X. Lu, and J. Zhang, *Phys. Rev. Lett.* **96**, 025003 (2006).
- [23] G. I. Stegeman and M. Segev, *Science* **286**, 1518 (1999), and references therein.
- [24] A. A. Ishaaya, T. D. Grow, S. Ghosh, L. T. Vuong, and A. L. Gaeta, *Phys. Rev. A* **75**, 023813 (2007), and references therein.
- [25] W. Liu and S. L. Chin, *Opt. Express* **13**, 5750 (2005).
- [26] B. La Fontaine *et al.*, *Phys. Plasmas* **6**, 1615 (1999).
- [27] S. L. Chin *et al.*, *Appl. Phys. B* **74**, 67 (2002).
- [28] G. Méchain *et al.*, *Appl. Phys. B* **79**, 379 (2004); *Opt. Commun.* **247**, 171 (2005).
- [29] Z. Hao *et al.*, *Opt. Express* **14**, 773 (2006); *Phys. Rev. E* **74**, 066402 (2006).
- [30] R. Y. Chiao *et al.*, *Phys. Rev. Lett.* **13**, 479 (1964).
- [31] K. D. Moll, A. L. Gaeta, and G. Fibich, *Phys. Rev. Lett.* **90**, 203902 (2003).
- [32] C. Ruiz *et al.*, *Phys. Rev. Lett.* **95**, 053905 (2005).
- [33] S. L. Chin *et al.*, *Laser Phys.* **18**, 962 (2008); Y. Chen *et al.*, *Opt. Lett.* **32**, 3477 (2007).
- [34] L. Bergé *et al.*, *Phys. Rev. Lett.* **92**, 225002 (2004).
- [35] S. Skupin *et al.*, *Phys. Rev. E* **70**, 046602 (2004).
- [36] R. Salamé *et al.*, *Appl. Phys. Lett.* **91**, 171106 (2007), and references therein.
- [37] A. Houard *et al.*, *Phys. Rev. A* **78**, 033804 (2008), and references therein.
- [38] Y.-Y. Ma *et al.*, *Opt. Express* **16**, 8332 (2008).
- [39] D. E. Roskey *et al.*, *Appl. Phys. B* **86**, 249 (2007).
- [40] M. Mlejnek, M. Kolesik, J. V. Moloney, and E. M. Wright, *Phys. Rev. Lett.* **83**, 2938 (1999).
- [41] L. Bergé, *Phys. Rep.* **303**, 259 (1998).